molecular pharmaceutics

articles

Stability of the *Clostridium botulinum* Type A Neurotoxin Complex: An Empirical Phase Diagram Based Approach

Duane T. Brandau,[†,‡,⊥] Sangeeta B. Joshi,[†,‡] Aaron M. Smalter,[†] Seonyoung Kim,[§] Bryan Steadman,[∥] and C. Russell Middaugh*[,†]

Department of Pharmaceutical Chemistry, 2030 Becker Drive, University of Kansas, Lawrence, Kansas 66047, Monsanto Company, 800 North Lindbergh Boulevard, St. Louis, Missouri 63167, and LigoCyte Pharmaceuticals, Inc., 2155 Analysis Drive, Bozeman, Montana 59718

Received December 13, 2006; Revised Manuscript Received March 9, 2007; Accepted April 23, 2007

Abstract: *Clostridium botulinum* type A neurotoxin (BoNT/A complex) is of great interest to the pharmaceutical industry. The drug itself is a natural complex of the toxin and a number of associated proteins. Surprisingly, relatively little is known about the exact structure and stability of the 900 kDa BoNT/A complex and its component proteins with the exception of the 150 kDa neurotoxin. In this study we describe the relative stability of the BoNT/A complex, the neurotoxin, and its associated proteins over a wide range of temperature and pH employing circular dichroism, intrinsic and 8-anilino-1-naphthalene sulfonate (ANS) fluorescence, and static light scattering. The data suggest a strong stabilizing effect of the associated proteins on the neurotoxin component. This data is compiled into empirical phase diagrams which permit the simultaneous visualization of multiple data sets over a wide range of conditions.

Keywords: Botulinum toxin A; physical stability; phase diagram

Introduction

Botulinum A toxin is one of seven serotypes (A−G) produced by the anaerobic bacteria *Clostridium botulinum*. These toxins are responsible for four recognized types of human diseases including infant botulism, wound botulism, and food-borne and adult intestinal colonization.[1,2] In all cases, the toxin, which is a Zn^{2+} endopeptidase, acts by blocking cholinergic synapses by cleaving intracellular proteins responsible for the docking and fusion of synaptic vesicles to the plasma membrane.[3] In the case of botulinum A toxin, the target is the SNAP 25 protein. The botulinum toxins are the most potent neurotoxins known with toxicity estimated to be 100 billion times more potent than cyanide. Despite this toxicity, botulinum toxins have been found to have great value as pharmaceutical agents and are currently used for the treatment of numerous disease states including achalasia, cerebral palsy, cervical dystonia, glabellar lines, headache, hyperhidrosis, musculoskeletal disorders, and spasticity among others.[4]

The botulinum A toxin is produced by the organism as a 900,000 MW complex consisting of 7 proteins including the active toxin.[5] The exact structure of the BoNT/A complex is not known, but it is composed of a group of hemagglutinating proteins and at least one non-hemagglutinating

* Address correspondence to this author. Mailing address: Pharmaceutical Chemistry, University of Kansas, 2030 Becker Dr., Lawrence, KS 66047. Tel: 785-864-5813. Fax: 785-864-5814. E-mail: middaugh@ku.edu.

† University of Kansas.

‡ These authors contributed equally to this work.

§ Monsanto Company.

⊥ Present address: Children's Mercy Hospital, 2401 Gillham Road, Kansas City, MO 64108.

∥ LigoCyte Pharmaceuticals, Inc.

(1) Cherington, M. Botulism: update and review. *Semin. Neurol.* **2004**, *24*, 155−163.

(2) Fox, C. K.; Keet, C. A.; Strober, J. B. Recent advances in infant botulism. *Pediatr. Neurol.* **2005**, *32*, 149−154.

(3) Bajohrs, M.; Rickman, C.; Binz, T.; Davletov, B. A molecular basis underlying differences in toxicity of botulism serotypes A and E. *EMBO Rep.* **2004**, *5*, 1090−1095.

(4) Munchau, A.; Bhatia K. P. Uses of botulism toxin injection in medicine today. *BMJ* **2000**, 320, 161−165.

10.1021/mp0601244 CCC: $37.00 **© 2007 American Chemical Society**
Published on Web 06/07/2007

polypeptide. These proteins have been hypothesized to function in the transport and protection of the toxin through the pH extremes of the GI tract prior to absorption of the neurotoxin.[6] Little else is known, however, about the structural relationships of the proteins that comprise the BoNT/A complex. Evidence suggests that the 150 kDa toxin is associated with one of the hemagluttinating proteins (HA-35) with a K_d of approximately 4×10^{-5}.[7,8] The non-hemaggluttinating protein appears to be degraded at acidic pH, and the 150 kDa toxin dissociates from the BoNT/A complex in basic solutions at pH 8.[6] This is in the range of intestinal pH where the toxin is probably absorbed and then transported through the circulation to target neurons.

From a medical, pharmaceutical, and physiological point of view, the physical stability of the neurotoxin and its associated proteins is of significant interest. We have utilized an empirical phase diagram approach[9,10] to examine and compare the physical stability of the BoNT/A complex, associated proteins, and neurotoxin over a wide range of pH and temperature conditions. In this instance, circular dichroism (CD), intrinsic and ANS fluorescence, and static light scattering (SLS) are used to examine the behavior of the BoNT/A complex, the neurotoxin, and associated proteins. We find significant differences in stability of the BoNT/A complex, associated proteins, and neurotoxin that suggest a strong stabilizing effect of the associated proteins on the neurotoxin component. The increased stability of the BoNT/A complex (neurotoxin complex) probably results from direct interactions among the associated proteins and neurotoxin.

Experimental Procedures

Materials. The BoNT/A complex (holotoxin, HT) was obtained from Allergan, Inc. (Irvine, CA), as an ammonium sulfate (1 M) suspension and stored at 4 °C. The ammonium sulfate suspension contained BoNT/A complex at 1.86 mg/mL in 33 mM sodium phosphate buffer at pH 6.0. The isoelectric point (p*I*) of the complex was 5.6. Stock solutions of the neurotoxin (NT) and the associated proteins (NAPs) were obtained from Metabiologics, Inc. (Madison, WI), in 20 mM sodium phosphate buffer, pH 7 at a concentration of 1 mg/mL. The isoelectric points (p*I*) of the NT and NAPs were 6.1 and 5.8, respectively. Reducing SDS−PAGE performed by Metabiologics, Inc., showed single bands at 100 and 50 kDa for the neurotoxin (NT) and 7 bands for the associated proteins (NAPs) (data not shown). All other chemicals were of reagent grade and were obtained from Sigma (St. Louis, MO) and Fisher Scientific (Pittsburgh, PA).

Methods. Protein Sample Preparation. The solutions of BoNT/A complex (HT) at different pH values were prepared in 50 mM citrate buffer containing 20 mM NaCl by dialyzing stock solutions into buffers ranging from pH 3 to 8, at one pH unit intervals. The dialysis was carried out overnight at room temperature in a biological safety cabinet. The concentration of the complex after dialysis was measured by UV absorption spectroscopy (A_{278} nm, $E_{1cm}^{0.1\%} = 1.66$)[11] after diluting the toxin complex (10-fold) in prefiltered citrate buffer at the desired pH values. The samples of BoNT/A complex at pH 5 could not be prepared by dialysis. The resulting solution was cloudy and exhibited a high degree of scattering as detected by turbidity measurements at 350 nm. To overcome this limitation, samples of BoNT/A complex at pH 5 were prepared by diluting a concentrated stock solution of BoNT/A complex at pH 6 (>2 mg/mL) into citrate buffer at pH 5, where the dilution factor was at least 20-fold. Samples of BoNT/A complex at various pH values were also diluted (10- to 20-fold) for CD, SLS, and intrinsic and ANS fluorescence measurements.

Working protein solutions of the neurotoxin and its associated proteins (0.05 mg/mL) for fluorescence measurements at different pH values were prepared by diluting the stock solutions of NT and NAPs (1 mg/mL) into 50 mM citrate buffer containing 20 mM NaCl at pH 3, 4, 5, 6, 7, and 8, with a dilution factor of 20. Because the extinction coefficient for the NT is approximately the same as that of BoNT/A complex ($E_{1cm}^{0.1\%}$ at 278 nm = 1.63)[12] and the value for the NAPs is not known, we used a value of 1.65 for this mixture of proteins. For CD studies, the stock solutions of NT and NAPs were concentrated using Centricon filters (MWCO-10k) to obtain 4 mg/mL solutions. The samples for CD were then prepared by diluting the concentrated stock (4 mg/mL) 20-fold into 50 mM citrate buffer, 20 mM NaCl at the desired pH to achieve a final protein concentration of 0.2 mg/mL. The neurotoxin (NT) and NAPs were also mixed at a 1:1 mole ratio, and CD and fluorescence studies were performed on this mixture with the final protein concentration the same as that employed in the other experiments. All

(5) Inoue, K.; Fujinaga, Y.; Watanabe, T.; Ohyama, T.; Takeshi, K.; Moriiishi, K.; Nakajima, H.; Inoue, K.; Oguma, K. Molecular Composition of *Clostridium botulinum* type A progenitor toxins. *Infect. Immun.* **1996**, *64*, 1589−1594.

(6) Chen, F.; Kuziemko, G. M.; Stevens, R. C. Biophysical characterization of the stsability of the 150-kilodalton botulinum toxin, the nontoxic component, and the 900-kilodalton botulinum toxin complex species. *Infect. Immun.* **1998**, *66*, 2420−2425.

(7) Fu, F.; Sharma, S. K.; Singh, B. R. A protease-resistant novel hemagglutinion purified from type A *Clostridium botulinum. J. Protein Chem.* **1998**, *7*, 53−60.

(8) Sharma, S. K.; Singh, B. R. Enhancement of the endopeptidase activity of purified botulinum neurotoxins A and E by an isolated component of the native neurotoxin associated proteins. *Biochemistry* **2004**, *43*, 4791−4798.

(9) Kueltzo, L. A.; Ersoy, B.; Ralston, J. P.; Middaugh, C. R. Derivative absorbance spectroscopy and protein phase diagrams as tools for comphrehensive protein characterization: a bBGSF case study. *J. Pharm. Sci.* **2003**, *92*, 1805−1820.

(10) Fan, H.; Ralston, J.; DiBase, M.; Faulkner, E.; Middaugh, C. R. The solution behavior of IFN-β-1a: An empirical phase diagram approach. *J. Pharm. Sci.* **2005**, *94*, 1893−1911.

(11) Stefanye, D.; Schantz, E. J.; Spero, L. Amino acid composition of crystalline botulinum toxin, type A. *J. Bacteriol.* **1967**, *94* (1), 277−278.

(12) Knox, J. N.; Brown, W. P.; Spero, L. Molecular weight of type A botulinum toxin. *Infect. Immun.* **1970**, *1* (2):205−206.

samples were prepared and experiments performed in a licensed BSL-3 facility.

Circular Dichroism. CD studies were performed with a Jasco J-810 spectropolarimeter equipped with a 6-position Peltier temperature controller. The CD signals of the proteins and protein complexes (0.2 mg/mL) were monitored at 222 nm every 0.5 °C at various pH values as a function of temperature from 12 to 90 °C. A scanning rate of 15 °C/h was employed using 0.1 cm path length cuvettes sealed with Teflon stoppers. The CD signals were converted to molar ellipticity using Jasco Spectra Manager software. Triplicate runs were performed for each study. The standard error was within 1.0%.

Intrinsic Fluorescence. Intrinsic fluorescence emission spectra of BoNT/A complex at 0.1 mg/mL, as well as NT and NAPs at 0.05 mg/mL, were recorded as a function of temperature (12−84 °C) and pH (3−8) using a PTI Quanta Master spectrophotometer equipped with a four-position temperature-controlled cell holder. The intrinsic fluorescence spectrum of tryptophan was monitored using an excitation wavelength of 295 nm (>95% Trp emission). Emission spectra were collected over a range of 300 to 400 nm. Excitation and emission slits were set at 4 nm, and a 1 cm path length quartz cuvette was used in all experiments. The spectra were collected at 3 °C intervals with a 5 min equilibration time at each temperature. Buffer baselines were subtracted from each spectrum prior to data analysis, which was performed using Felix (PTI) and Origin 6 software. Emission peak positions were determined by a center of spectral mass method because of better wavelength reproducibility. Thus, the reported values do not correspond to actual peak positions (they are approximately 10−14 nm red-shifted), but do directly reflect shifts in peak positions. Triplicate runs were performed for each study. The standard error was within 0.5%.

ANS Fluorescence. The compound 8-anilino-1-naphthalene sulfonate (ANS, Sigma) was used as an extrinsic fluorescent probe to study alterations in tertiary structure. The interaction of ANS with BoNT/A complex, NT, and NAPs was monitored as a function of temperature (12−84 °C) and pH (3−8) using the PTI Quanta Master spectrophotometer. The concentration of protein employed was again 0.1 mg/mL for BoNT/A complex and 0.05 mg/mL for NT and NAPs. A molar ratio of ANS to protein of 100:1 was employed in all experiments. An excitation wavelength of 372 nm was used, and spectra were collected from 400 to 600 nm. Excitation and emission slits were set at 4 nm, and 1 cm path length quartz cuvettes were used. The spectra were again collected at 3 °C intervals with a 5 min equilibration time at each temperature. Triplicate experiments were performed for each study. The standard error was within 1.0%.

Static Light Scattering Measurements. Static light scattering measurements were performed using the PTI fluorometer at protein concentrations of 0.1 mg/mL for BoNT/A complex and 0.05 mg/mL for both neurotoxin and associated proteins. Five measurements were obtained of the scattering intensity at 350 nm and averaged for each pH and temperature point. The standard error was within 0.5%. Like the previous thermal melts, data was obtained over the pH range of 3 to 8 and temperatures from 12 to 84 °C in 3 °C increments.

Construction of Empirical Phase Diagrams. Empirical phase diagrams were constructed as described previously[9,10] employing CD molar ellipticity, intrinsic Trp fluorescence intensity, and ANS fluorescence intensity data. SLS data was found to have little effect on the phase diagrams and was not included in their construction. All calculations were performed using MATLAB software (The Mathworks Inc., Natick, MA). Briefly, experimental data sets are represented as *n*-dimensional vectors in a temperature/pH phase space, where *n* refers to the number of variables (different types of data, 3 in this case) included in the calculation. The data from each technique at individual values of pH and temperature serve as the basis for the individual vector's components. After normalization of the data to values between 0 and 1, an $n \times n$ density matrix combining all of the individual vectors is then constructed and *n* sets of eigenvalues and eigenvectors of the density matrix are calculated. The phase diagram is then generated using colors generated by a MATLAB function employing an arbitrary red/green/blue color scheme.

Results

150 kDa Neurotoxin (NT). In this study, the neurotoxin component of the BoNT/A complex was characterized by thermal unfolding (T_ms) studies using circular dichroism, intrinsic and extrinsic (ANS) fluorescence spectroscopy, and 90° static light scattering measurements. The unfolding and aggregation of NT showed a complicated dependence on pH and temperature. At pH 3, unfolding was multiphasic as determined by monitoring the molar ellipticity at 222 nm (Figure 1A). An initial decrease (more negative) in molar ellipticity was observed at 30 °C to 50 °C, beyond which a gradual increase occurred up to 90 °C. In contrast, CD melting curves for pH 4 to 8 showed sharp transitions with T_m values ranging from 50 to 52 °C, although at pH 4 the transition occurred over a much wider temperature range (∼20 °C) (Figure 1A). Increases in ellipticity at 222 nm are consistent with a loss of α helical and, to a lesser extent, β sheet structure and the appearance of a disordered state. Although some of the observed transitions were multiphasic, the "apparent" transition temperatures (T_m^*) were obtained as midpoints of total change from sigmoidal fits of the data (Table 1). CD spectra obtained at each pH prior to thermal unfolding showed peak minima at approximately 215 nm (data not shown). At pH 3, however, the molar ellipticity becomes more negative with increasing temperature while from pH 4 to 8 the molar ellipticity becomes less negative suggesting that at low pH the neurotoxin undergoes intermolecular β-sheet formation with increasing temperature consistent with microaggregation (see below).

The binding of the dye ANS to apolar sites on proteins is often associated with an enhanced fluorescence and a blue

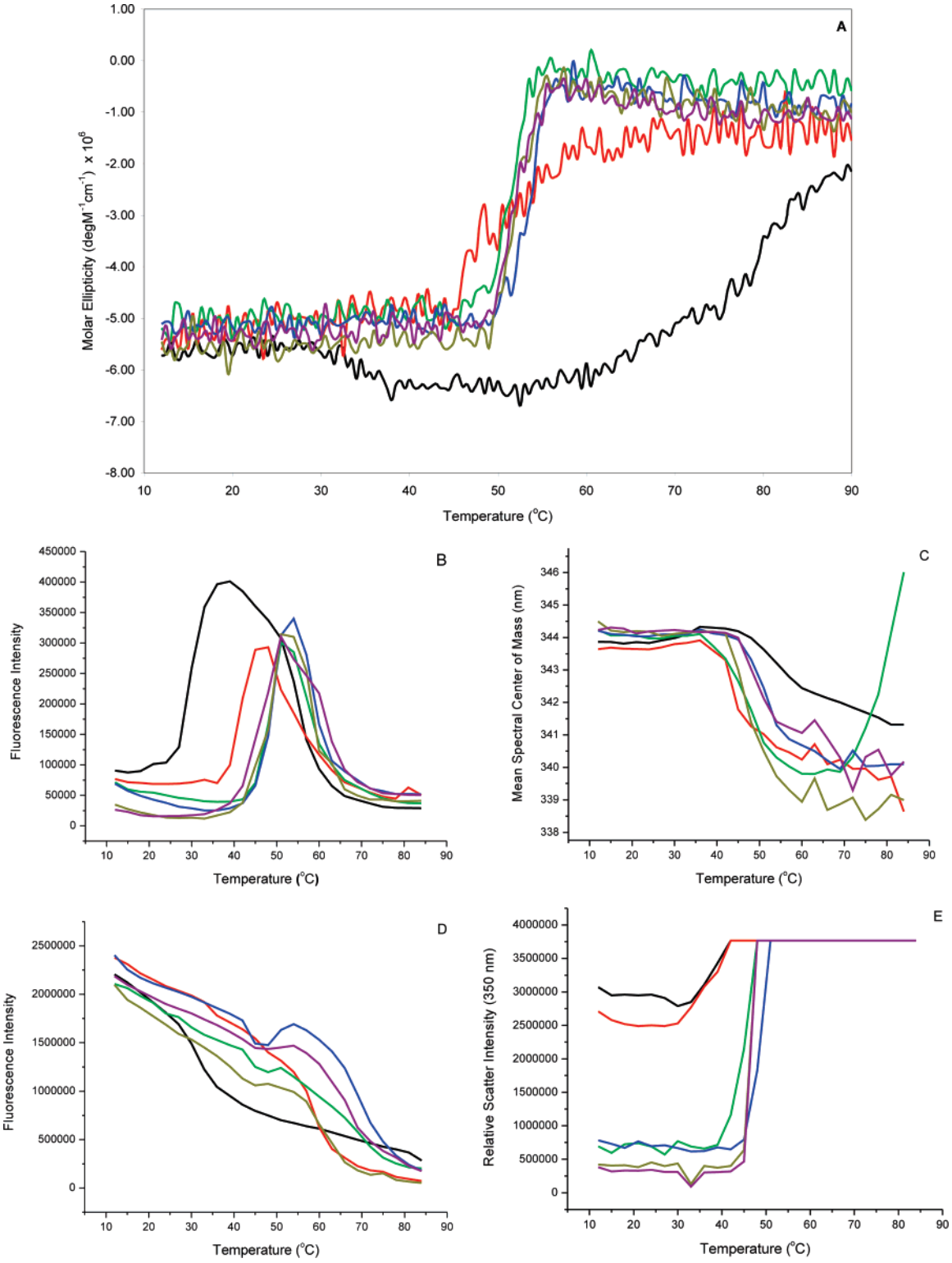

Figure 1. Characterization of 150 kDa neurotoxin as a function of temperature and pH. (A) Circular dichroism: ellipticity at 222 nm. (B) ANS fluorescence emission intensity. (C) Intrinsic fluorescence: tryptophan peak wavelength shift. (D) Intrinsic fluorescence emission intensity. (E) Static light scattering: intensity at 350 nm. All experiments were conducted in a 50 mM citrate buffer containing 20 mM NaCl. For all the plots, pH 3 (black), pH 4 (red), pH 5 (green), pH 6 (blue), pH 7 (gold), and pH 8 (purple).

shift in the dye's wavelength of peak emission. In some cases, the negative charge on the ANS is also thought to be involved in its interaction with proteins.[13] ANS is also generally considered to have a much stronger affinity for

Table 1[a]

	NT and NAPs transition midpoint (° C)					
	CD		intrinsic fluorescence		ANS fluorescence	
pH	NT	NAPs	NT	NAPs	NT	NAPs
3	34.1	73.0	58.1	nd[b]	30.2	54.2
4	50.2	63.6	47.2	nd	42.1	59.1
5	51.2	63.1	47.4	nd	47.8	60.1
6	53.3	64.0	52.1	nd	48.9	54.2
7	52.4	62.1	48.3	nd	48.1	54.8
8	52.1	61.6	52.2	nd	46.2	52.0

	BoNT/A complex transition midpoint (°C)		
	CD	intrinsic fluorescence	ANS fluorescence
3	66.8	68.8	56.9
4	65.5	nd	61.2
5	63.5	nd	63.0
6	58.5	nd	52.9
7	56.7	67.8	48.2
8	55.9	69.0	42.0

[a] Standard errors for all runs were approximately ±0.5 °C. [b] Not determined due to small transition.

protein "molten globule" states than for native and strongly structurally disrupted conformational forms.[14]

Changes in ANS fluorescence intensity of the neurotoxin as a function of temperature and pH are shown in Figure 1B. Sharp transitions at each pH are apparent, and the resultant T_m^* values (Table 1) indicate that the NT is most stable between pH 5 and 7. The maximum intensity of ANS fluorescence occurred at 39 °C for pH 3, 48 °C for pH 4, and between 51 and 54 °C for pH 5−8. The shift to higher temperatures with increasing pH parallels that seen with CD although the T_ms determined by ANS fluorescence are uniformly lower than those detected by CD measurements. Such differences suggest molten globule like behavior of the toxin at all pH values.

Changes in a protein's intrinsic fluorescence are typically sensitive to tertiary structure alterations as well as secondary structure changes. The change in mean fluorescence spectral center of mass of the NT showed a pronounced blue shift at all pH values at elevated temperature, suggesting that the protein's tryptophan side chains are in a more apolar environment upon structural perturbation (Figure 1C). The transition occurred at higher temperature (∼50 °C) for pH 3 compared to other pH values (36−45 °C). Plots of intrinsic fluorescence intensity for pH 3 and 4 showed a downward sigmoidal transition with increasing temperature while at pH 5−8 a biphasic transition is observed with a slight increase in fluorescence intensity over a 10 to 15 deg temperature range (Figure 1D).

Static light scattering measurements of the 150 kDa toxin suggest changes in size for the toxin as a function of pH at temperatures below 30 °C (Figure 1E). At pH 3 and 4 the relative scattering intensity was significantly higher than at pH 5−8 and notable differences were observed between pH 5−6 and 7−8 as well. The temperatures at which aggregation occurred also displayed temperature dependence with lower pH values aggregating at lower temperatures compared to pH 7−8 while aggregation at pH 5−6 was intermediate. This trend is similar to that seen with the CD and ANS fluorescence studies and strongly suggests decreased thermal stability at lower pH values for the neurotoxin.

The empirical *T*/pH phase diagram constructed from CD, intrinsic fluorescence, and ANS fluorescence intensity data for the neurotoxin is shown in Figure 2. It appears that this protein adopts at least five different states. The yellow-green region up to approximately 27 °C at pH 3, 40 °C at pH 4, and 50 °C at pH 5 to 8 appears to be the phase of maximum stability (Figure 2) based on CD and ANS fluorescence measurements. As anticipated, the midpoints of the transitions observed by the spectral measurements generally correspond to the pseudo-phase boundaries. The pink-purple region in the pH range 4 to 8 from 40 to 60 °C appears to represent protein with significant molten globule character. A third phase (blue-white) is present at pH 4−8 in the higher temperature region. This depicts a phase in which the protein is extensively unfolded and tends to aggregate. Another phase (dark purple) is apparent at pH 3 at temperatures between 30 and 55 °C. In this state, the neurotoxin manifests more exposed apolar sites suggesting partial unfolding prior to aggregation which may again involve the presence of molten globule-like states. A final phase is identifiable at temperatures above 55 °C (green) at pH 3 which we assume corresponds to even more structurally disrupted forms based on spectral measurements.

Neurotoxin Associated Proteins (NAPs). The NAPs were studied in the same manner as the neurotoxin using the same techniques and range of variables. Thermal melts as a function of pH obtained by monitoring molar ellipticity at 222 nm showed a transition at 73 °C at pH 3 while at pH 4−8 the transitions occurred between 61 and 65 °C (Figure 3A). Additionally, the initial molar ellipticities at 12−50 °C ranged from -4.0×10^6 to -1.4×10^7 deg M^{-1} cm^{-1}, suggesting major differences in secondary structure as a function of pH for the NAPs (Figure 3A).

ANS fluorescence studies of the NAPs show a striking pH dependence at low temperature (<45 °C) followed by an increase in ANS fluorescence with increasing temperature at all pH values (Figure 3B). Most notably there is a 3-fold decrease in intensity from 12 to 45 °C at pH 4 followed by an increase in intensity that remains less than that seen at 12 °C. At pH 7 and 8 there is a slight increase then decrease in intensity prior to the sharp increase beginning at 35 °C. ANS intensity decreases slightly at pH 3 and 5 before

(13) Matulis, D.; Lovrien, R. 1-Anilino-8-naphthalene sulfonate anion-protein binding depends primarily on ion pair formation. *Biophys. J.* **1998**, *74* (1), 422−429.

(14) Semisotnov, G. V.; Rodionova, N. A.; Razgulyaev, O. I.; Uversky, V. N.; Gripas, A. F.; Gilmanshin, R. I. Study of the "molten globule" intermediate state in protein folding by a hydrophobic fluorescent probe. *Biopolymers* **1991**, *31*, 119−128.

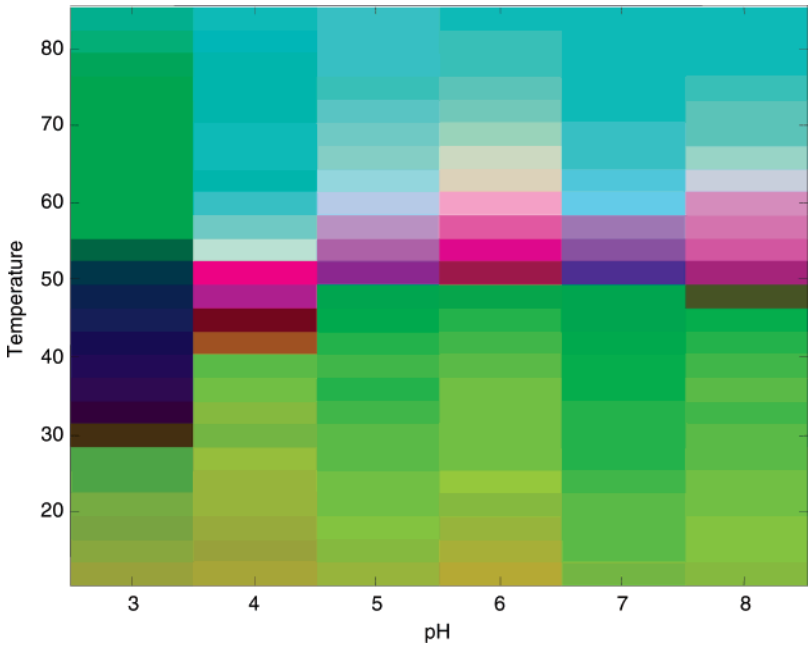

Figure 2. Temperature−pH phase diagram of neurotoxin based on CD intensity, ANS fluorescence intensity, and intrinsic fluorescence intensity data. The data employed to generate these images was obtained over the pH range of 3 to 8 and temperatures from 12 to 84 °C in 3 °C increments. Blocks of continuous color represent conditions under which the raw data-derived vectors behave similarly.

increasing at 39 °C and 45 °C, respectively. The variation in ANS intensities is thought to arise from the heterogeneity of the NAPs due to the presence of multiple proteins.

Intrinsic fluorescent peak positions determined by mean spectral center of mass (Figure 3C) remain constant at all pH values until 51 °C, where the data at pH 3 shows a slight blue shift followed by a red shift at 69 °C, followed by another red shift at higher temperatures. The NAPs at pH 4 undergo a blue shift of 2 nm from 51 °C to 69 °C followed by a similar pattern at pH 3. The proteins at pH 5 also undergo a slight blue shift followed by a red shift above 70 °C. At pH 6, a very slight blue shift (∼1 nm) is followed by a red shift above 70°. NAPs at pH 7 and 8 show a gradual red shift above 51 °C, suggesting disassociation of the NAPs or an unfolding of the individual proteins. Measurements of fluorescence intensity show a uniform decrease in intensity for all pH values until approximately 60 °C, where intensity decreases much more rapidly (Figure 3D).

Static light scattering measurements of the NAPs were obtained from 12 to 84 °C (Figure 3E). At all pH values, scattering intensity slightly decreases from 12 to 48 °C and then rises sharply between 45 and 66 °C over the entire pH range. At pH 3 and 4, the scattering intensity begins to increase between 45 and 50 °C, while at pH 5 and 6 the onset of rapid increase in scattering intensity occurs above 57 °C. For NAPs at pH 7 and 8, the transition point occurs at 51 and 48 °C, respectively.

The empirical phase diagram (Figure 4) of the NAPs demonstrates quite heterogeneous behavior as might be expected from a mixture of proteins. No clearly defined phase boundaries are present except a purple-blue phase at higher temperatures that probably reflects major protein conformational changes and aggregation based on the light scattering and spectral measurements.

BoNT/A Complex (HT). The secondary structure of the BoNT/A complex, as determined by CD thermal studies while monitoring molar ellipticity at 222 nm, undergoes significant pH and temperature-dependent changes (Figure 5A). Below 50 °C, there are significant differences in molar ellipticity for the complex ranging from −50 to −15 × 10^6 deg M^{-1} cm^{-1}, suggesting pH dependent structural changes below 50 °C. Above 50 °C, the molar ellipticity at all pH values with the exception of pH 3 become less negative. The HT at pH 3 shows increasingly more negative molar ellipticity, suggesting a significantly different secondary structure at this pH. Although most transitions were multiphasic as expected for a large protein complex, the "apparent" transition temperatures (T_m^*) were obtained as midpoints of total change from sigmoidal fit of the data (Table 1). The transitions occur at lower temperatures at higher pH values (pH 6−8), suggesting that the BoNT/A complex is structurally more labile above pH 6.

The changes in ANS fluorescence intensity of the BoNT/A complex as a function of temperature and pH are shown in Figure 5B. Unlike the NAPs, ANS intensity of the HT displays little change at all pH values until 40 °C. Above 40 °C a series of sharp increases in ANS fluorescence is noted. The resultant T_m^* values (Table 1) indicate that the BoNT/A complex is most stable between pH 4 and 5. The complex appears to be significantly destabilized between pH 6 and 8 since the corresponding transitions occur at much lower temperatures.

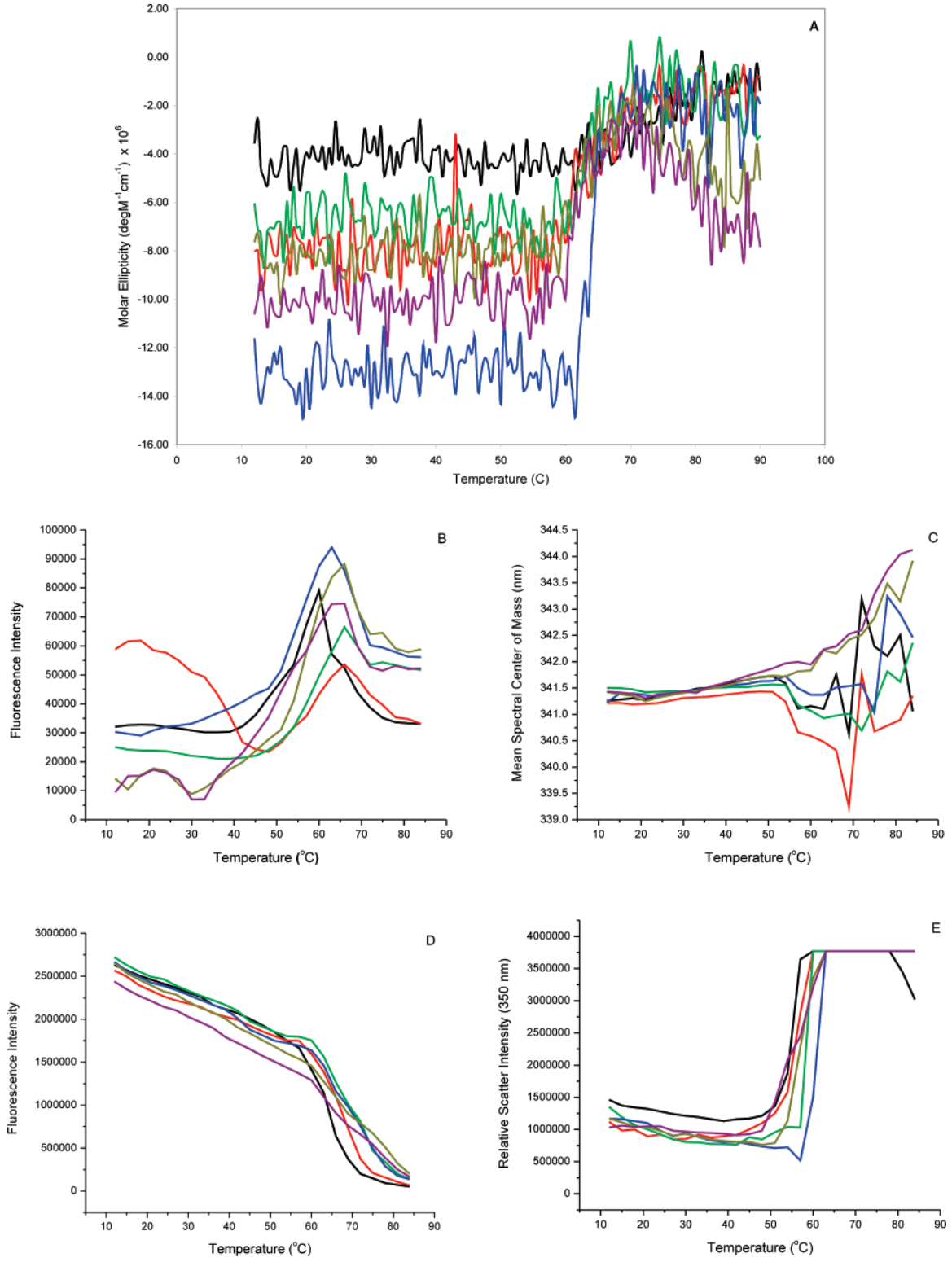

Figure 3. Characterization of neurotoxin associated proteins (NAPs) as a function of temperature and pH. (A) Circular dichroism: ellipticity at 222 nm. (B) ANS fluorescence emission intensity. (C) Intrinsic fluorescence: tryptophan peak wavelength shift. (D) Intrinsic fluorescence emission intensity. (E) Static light scattering: intensity at 350 nm. All experiments were conducted in a 50 mM citrate buffer containing 20 mM NaCl. For all the graphs, pH 3 (black), pH 4 (red), pH 5 (green), pH 6 (blue), pH 7 (gold), and pH 8 (purple).

The effect of pH and temperature on the conformational stability of the BoNT/A complex was also monitored using intrinsic tryptophan fluorescence measurements. The change in mean spectral center of mass as a function of temperature and pH is shown in Figure 5C. No significant change in peak position is noted until temperatures above 57 °C where red

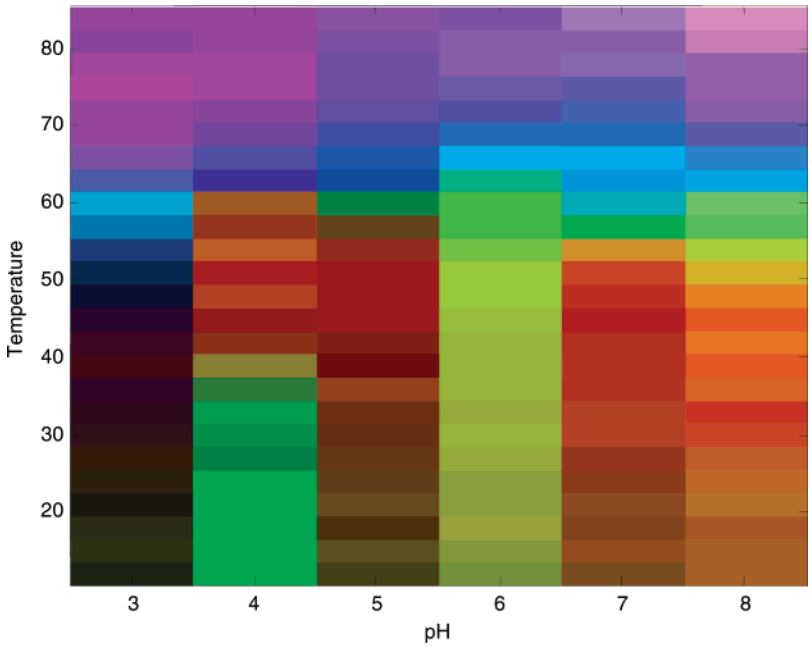

Figure 4. Temperature−pH phase diagram of neurotoxin associated proteins (NAPs) based on CD intensity, ANS fluorescence intensity, and intrinsic fluorescence intensity data. The data employed to generate these images was obtained over the pH range of 3 to 8 and temperatures from 12 to 84 °C in 3 °C increments. Blocks of continuous color represent single phases, conditions under which the raw data-derived vectors behave similarly.

shifts are noted for pH 3, 6, 7, and 8. Such shifts are conventionally taken to reflect an increase in exposure of a protein's indole side chains. In contrast, a small blue shift (∼ 1 nm) in the peak positions was observed at pH 4 and 5. The maximum emission wavelength versus temperature curves for BoNT/A complex (Figure 5D) demonstrate a typical decrease in intensity with temperature at all pH values with small but marked transitions occurring at different temperatures for different pH values. At pH 5, the fluorescence intensity of the BoNT/A complex at the peak maximum was significantly lower compared to other pH values. At all pH values, the presumptive changes in tertiary structure of the complex, as suggested by the shifts in intrinsic tryptophan fluorescence peaks, commence at temperatures higher than secondary structural changes or apolar character as measured by CD and ANS fluorescence, respectively (Table 1). This is in contrast to what is generally observed with most proteins in which tertiary structure changes usually occur prior to any secondary structure alterations.[15] This presumably reflects the complexity of the toxin complex and its solution behavior. It may also be the case that the intrinsic fluorescence data reflect something other than tertiary structural changes (e.g., alterations in quaternary structure).

Static light scattering measurements as a function of temperature and pH were also obtained for the BoNT/A complex and are shown in Figure 5E. Little change in scattering intensity is noted below 50 °C. At pH 4, a sharp increase in scattering intensity is observed followed by increased scattering at pH 5, 6, 3, 7, and 8 with increasing temperature.

The empirical phase diagram for the BoNT/A complex was constructed from CD, intrinsic fluorescence, and ANS fluorescence intensity data sets. The phase diagram of the BoNT/A complex (Figure 6) shows at least five phases and includes a unique state at pH 5 not seen in the other phase diagrams (Figures 2 and 4). The properties of the protein within each phase can be established by reference to the individual measurements. At pH 3 and 4, the BoNT/A complex appears to be in a similar structural state (reddish-brown) characterized by little exposure of apolar sites and buried tryptophan residues and remains in the same state up to approximately 55 °C at pH 3 and 60 °C at pH 4. At more elevated temperatures at low pH, complex multistate behavior appears to occur (blue-green-purple). Another phase (purple) is apparent at pH 5. The reddish-brown region at pH 3 and 4 and the purple region at pH 5 represent the region of maximum stability based on these measurements. Although CD and ANS data suggest that the BoNT/A complex is fairly stable at pH 5 and might be expected to appear as a single phase at pH 3 and 4, the appearance of this new phase may be due to the decreased negative ellipticity of BoNT/A complex at lower temperatures. This suggests toxin components of different secondary structure that tend to form microaggregates at lower temperatures. A third phase (greenish-brown) appears to be present at pH 6, 7, and 8 up to 45−55 °C. CD and ANS data indicate decreased stability of BoNT/A complex at higher pH values compared to more acidic conditions. As the temperature increases, the complex rapidly enters another phase (green) above 50 °C at pH 6.

(15) Haynie, D. T.; Freire, E. Structural energetics of the molten globule state. *Proteins* **1993**, *16* (2), 115−140.

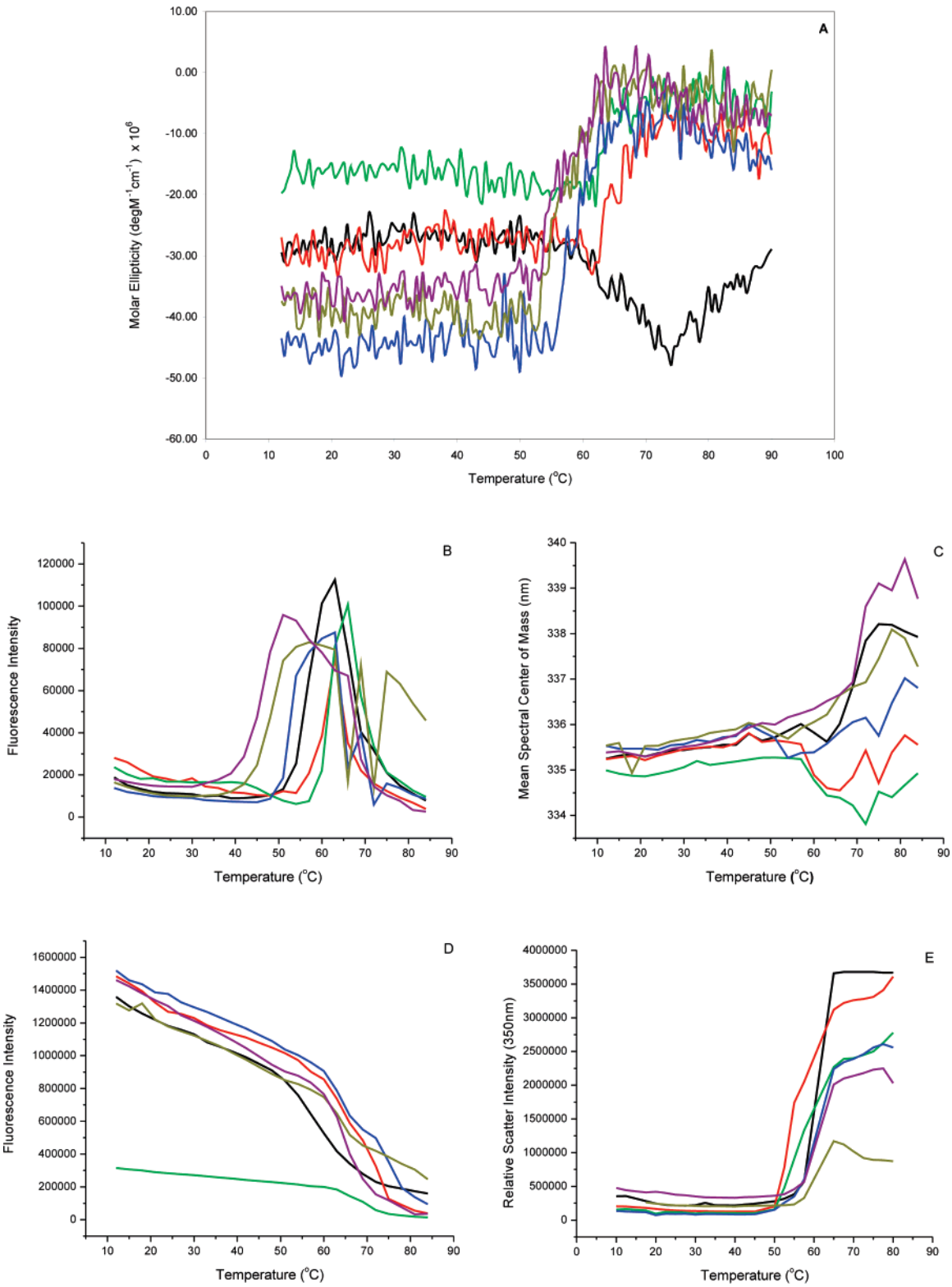

Figure 5. Characterization of BoNT/A complex as a function of temperature and pH. (A) Circular dichroism: ellipticity at 222 nm. (B) ANS fluorescence emission intensity. (C) Intrinsic fluorescence: tryptophan peak wavelength shift. (D) Intrinsic fluorescence emission intensity. (E) Static light scattering: intensity at 350 nm. All experiments were conducted in a 50 mM citrate buffer containing 20 mM NaCl. For all the graphs, pH 3 (black), pH 4 (red), pH 5 (green), pH 6 (blue), pH 7 (gold), and pH 8 (purple).

This region, which extends across pH 7 and 8 at temperatures above 45 °C, appears to represent protein with significant molten globule character based on spectral measurements. In this phase, the complex appears to possess exposed apolar

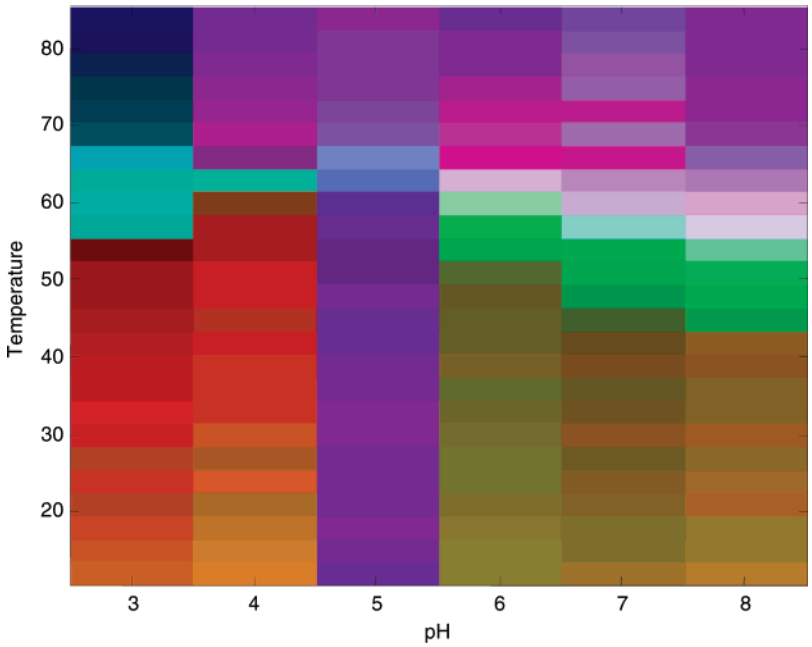

Figure 6. Temperature−pH phase diagram of BoNT/A complex based on CD intensity, ANS fluorescence intensity, and intrinsic fluorescence intensity data. The data employed to generate these images was obtained over the pH range of 3 to 8 and temperatures from 12 to 84 °C in 3 °C increments. Blocks of continuous color represent single phases, conditions under which the raw data-derived vectors behave similarly.

sites that result in aggregation at higher temperatures. An additional phase (blue-purple) in the higher temperature region over the entire pH range of 3 to 8 appears to result from protein that is severely structurally altered, and tends to aggregate.

Discussion

These studies permit for the first time a comparison of the physical stability of the BoNT/A complex, its associated proteins, and neurotoxin. The effects of temperature and pH on the structure of the polypeptides were obtained by employing circular dichroism, intrinsic fluorescence, ANS fluorescence, and SLS. Comparison of the effect of temperature on all three species shows the BoNT/A complex to be significantly more stable than the 150 kDa neurotoxin while the neurotoxin associated proteins display intermediate thermal stability. This conclusion is in agreement with previously published biological studies which suggest that the associated proteins protect the neurotoxin against the extremes of pH encountered by the toxin upon ingestion.[5,6] The greatest stability of the complex appears at lower pH (3−5) with the maximum stability seen at pH 4−5. CD temperature data at 222 nm for the complex shows decreased negative ellipticity at pH 5 which could result from increased aggregation (and possibly absorption flattening). Similarly, intrinsic fluorescence data at this pH is much less intense than at other pH values. Furthermore, sample preparation at pH 5 reveals visible turbidity after dialysis into pH 5 buffer. It is of note that one of the associated proteins (HA-33) can be purified from the BoNT/A complex complex at pH 5.5 by molecular sieve chromatography while the remainder of the complex stays intact. This suggests the possibility of molecular rearrangement of the complex at pH 5 to 6.[7] It has also been shown that NT binds to HA-33 at pH 7.4 ($k_d = 4 \times 10^{-5}$) with increased enzymatic activity. This supports the idea of a conformational change within the complex over the pH range of 4 to 7.[8]

Comparison of the CD and ANS fluorescence data suggests the possible existence of some molten globule-like character for the BoNT/A complex over the pH range of study. ANS fluorescence T_m* changes are 5 to 10 °C lower than corresponding changes in CD T_m* values at each pH. The exception is seen at pH 5 which shows only a degree difference. The lack of a molten globule behavior at pH 5 presumably reflects the increased stability of the complex at this pH. This is clearly seen in the empirical phase diagram of the BoNT/A complex (discussed below). Since the BoNT/A complex consists of 7 proteins, it is possible that this molten globule behavior reflects initial changes in apolar character resulting from molecular rearrangement and/or changes in the association state of the components of the complex, although dynamic light scattering measurements do not suggest dissociation of the holotoxin complex (HT) over the temperature and pH range of this study (data not shown).

Comparison of NT and HT thermal data by all techniques shows that the neurotoxin is thermally much less stable than the BoNT/A complex. At pH 3, T_m* values differ by over 30 °C and then become closer at higher pH. From pH 3 to 4, a significant 15 °C change is observed by CD, suggesting

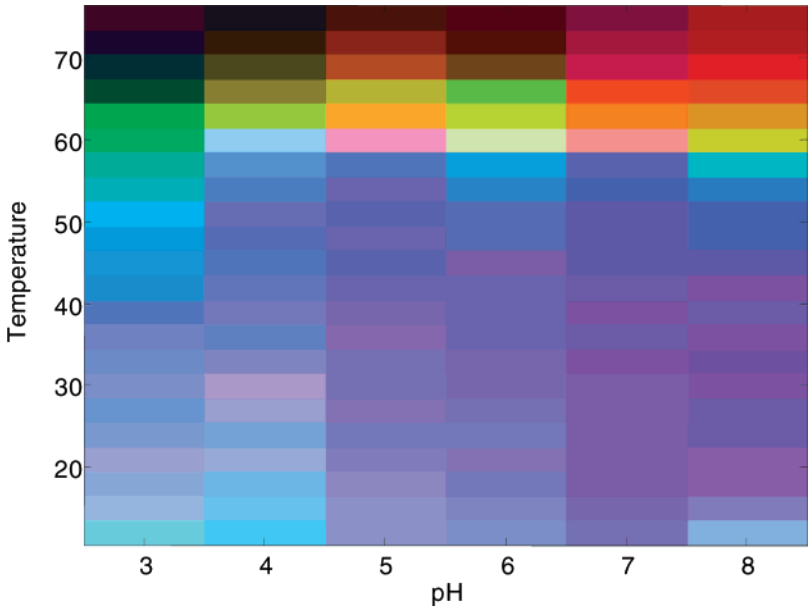

Figure 7. Temperature−pH phase diagram of NT + NAPs combination based on CD intensity, ANS fluorescence intensity, and intrinsic fluorescence intensity data. The data employed to generate these images was obtained over the pH range of 3 to 8 and temperatures from 12 to 75 °C in 3 °C increments. Blocks of continuous color represent conditions under which the raw data-derived vectors behave similarly.

a significant alteration in the secondary structure of the neurotoxin. This change may reflect the changes in the heavy chain component of the NT that occur in the endosome prior to release of light chain within neurons.[16] ANS fluorescence data also suggest changes in the apolar character of the neurotoxin over this pH range as the T_m* value changes from 30 °C to 42 °C from pH 3−5. Maximal thermal stability of the neurotoxin appears at pH 6 although the T_m* of the NT is 6 °C less than that of the BoNT/A complex as measured by CD. Comparison of CD and ANS fluorescence T_m*s for the neurotoxin clearly suggests a molten globule state over the entire pH range of this study. A similar observation has been reported by Kukreja and Singh[17] for the light chain of botulinum toxin A. This state is clearly observed in the empirical phase diagram of the NT as discussed below. Comparison of the T_m* values of NT and HT clearly indicates the increased stability and subsequent protection of the neurotoxin imparted by the associated proteins in the complex. This is evident from comparison of the T_m* values for the associated proteins to those of the BoNT/A complex and NT component. The T_m* values of the NAPs change over the pH range of this study and are much closer to those of the BoNT/A complex. While the CD and ANS thermal data also suggests the existence of molten globule states in the associated proteins, it is not as apparent in the phase diagram.

The empirical phase diagram of the associated proteins is much more heterogeneous than the BoNT/A complex or the neurotoxin. Clearly defined states other than the aggregation of the proteins above 60 °C are not discerned. This heterogeneous appearance undoubtedly reflects a "blurring out" of the individual behaviors of the associated proteins with the appearance of the NAPs phase diagram simply reflecting the sum of the individual proteins. To evaluate if addition of the neurotoxin back to the NAPs would restore the structure of the complex, a phase diagram of the combined associated proteins and neurotoxin in a 1:1 mole ratio was generated using the same experimental techniques and conditions employed for the BoNT/A complex phase diagram (Figure 7). This "combination" phase diagram manifests no clearly defined states, suggesting that simple addition of the components does not reconstitute the BoNT/A complex. Various combinations of NT and NAPs were tried without success to regenerate the BoNT/A complex phase diagram (data not shown). This result is not unexpected in that attempts to experimentally reconstitute the BoNT/A complex from components have generally been unsuccessful.[6]

In conclusion, the BoNT/A complex, associated proteins, and neurotoxin have been characterized over a wide range of pH in terms of their thermal stability by a variety of techniques, including CD, intrinsic fluorescence, and ANS. The BoNT/A complex displays increased thermal stability over the entire pH range studied in comparison to the neurotoxin component. This increased stability appears to arise from the internal structure of the complex generated by interactions between the neurotoxin and the associated proteins. Characterization of the BoNT/A complex reveals

(16) Li L.; Singh, B. R. Spectroscopic analysis of pH-induced changes in the molecular features of Type A botulinum neurotoxin light chain. *Biochemistry* **2000**, *39*, 6466−6474.

(17) Kukreja, R.; Singh, B. R. Biologically active novel conformational state of botulinum, the most poisonous poison. *J. Biol. Chem.* **2005**, *280* (47), 39346−39352.

dynamic structure that is probably related to the transport of the toxin through the GI tract. The increased stability of the 900 kDa holotoxin compared with the 150 kDa neurotoxin observed in this study may have direct relevance to the comparative stability of commercial preparations of botulinum toxin type A, which are diluted in isotonic saline and injected directly into patient tissue of pH and temperature within the ranges explored here. A preliminary potency comparison between a botulinum toxin type A formulation of the 900 kDa holotoxin and one of only the 150 kDa neurotoxin is consistent with the findings of this study, reaffirming the roles played by the neurotoxin associated proteins in protecting and stabilizing the 150 kDa neurotoxin.[18]

(18) Hunt, T.; Clarke, K. Substandard potency of Xeomin in the Botox mouse LD50 assay. *Mov. Disord.* **2006**, *21* (Suppl. 15), S348 ABS-P71.

Acknowledgment. Funding for this work was provided by Allergan, Inc.

MP0601244